

Fatigue Crack Growth and Life Descriptions of Sn3.8Ag0.7Cu Solder Joints: A Computational and Experimental Study

D. Bhate¹, D. Chan¹, G. Subbarayan¹, L. Nguyen²

¹School of Mechanical Engineering, Purdue University, West Lafayette, IN 47907-2088

²National Semiconductor Corporation, Santa Clara, CA 95051

Phone: (765) 494-9770

Fax: (765) 494-0539

Email: ganeshs@purdue.edu

Abstract

The need for predicting fatigue life in solder joints is well appreciated at the present time. Currently, however, there are very few experimentally validated material parameters for popular SnAgCu alloys. Furthermore, the validity of Coffin-Manson life models, being empirical, also needs to be explored for these alloys which creep in a manner significantly different from SnPb solder alloys. In this paper, we present a modeling approach inspired by cohesive zone theory of modern fracture mechanics and Weibull distributions of material failure. The approach relies on the accurate estimation of inelastic strains at the crack tip estimated through finite element analysis, which are then used to make decisions on crack propagation. Like most popular cohesive zone models, the modeling approach presented here requires the estimation of two parameters. Unlike most cohesive zone models however, no special elements are needed in the finite element model and estimation of the parameters is more straightforward. We demonstrate the applicability of the modeling approach via the simulation of fatigue crack growth in Sn3.8Ag0.7Cu solder joints subjected to anisotropic thermal cycling. Anisotropic thermal cycling conditions were created experimentally using a simulated power cycling testing device and fatigue crack fronts were tracked at different life cycles using traditional dye-and-pry methods. The experiments were repeated for varying temperature profiles. Experimental results were coupled with numerical analysis to obtain fracture parameters for Sn3.8Ag0.7Cu. The model and the parameters were then validated by verifying their predictive ability against a variety of temperature profiles. In a separate study, the authors have developed a time hardening creep model for describing the behavior of Sn3.8Ag0.7Cu. The time hardening model accounts for primary and secondary creep and does not restrict itself to the assumption of steady state creep. The need for accurate estimation of inelastic strains in the finite element model is thus met using a valid constitutive model to describe solder creep behavior. The ability of the model to predict three dimensional crack fronts for a variety of fatigue loading environments, with sufficient accuracy, is a key result of this work.

1. Introduction

Solder joint fatigue has been the subject of a great deal of study. The reason for this is easily understood on examining the nature of the problem: complex and non-standardized package geometries, variable environmental conditions that impose strong thermomechanical effects, and perhaps most

importantly, the material behavior of the solder alloys. The recently implemented alternatives to lead-based solder alloys differ from the eutectic Sn-Pb solders in their creep properties [1, 2] and the effects of aging [3], thereby introducing additional complexity. The microelectronic packaging industry primarily relies on the tried and trusted technique of imposing controlled thermal cycling on electronic packages in an experimental environment, estimating Weibull characteristic lives and shape parameters and relating this to empirical rules such as the Coffin-Manson rule and its variants [4]. It is common knowledge that this technique does not deal with the physics of the problem at hand; as such, predictions of fatigue life for different material systems and package geometries are not feasible unless thermal cycling tests are repeated for the various microelectronic packages under consideration.

Solder joint fatigue failure is, at its essence, a fatigue crack growth problem. It is therefore natural that a non-empirical understanding of this problem can only result from adopting a fracture mechanics framework. While linear elastic fracture mechanics (LEFM) does provide approaches such as the Paris law [5] that deal with fatigue crack growth, the assumptions made in these approaches are almost always not valid for studying crack growth in solder interconnections. This is primarily due to the fact that typical fatigue failures in solder involve large cracks (relative to pad size) and large scale plastic yielding, both of which invalidate the use of LEFM [6]. One of the reasons LEFM breaks down for this class of problems is because it does not explicitly deal with the specific nature of material degradation in the vicinity of the crack. It has been shown that fatigue crack propagation is the end result of accumulating degradation in front of the crack tip (a region called as the process zone) either in the form of microcracking (as observed in cementitious composites, for example) or formation and growth of voids (as observed in ductile materials including solder) [7].

Nonlinear fracture mechanics, which includes, but is not limited to, the critical crack tip opening angle (CTOA) method [8], the elastoplastic J-integral approach [9] and the cohesive zone model approach [10-14], has attempted to address the issues of large scale yielding and large cracks. The cohesive zone model has emerged as a popular approach primarily due to the fact that it separates material behavior in the process zone from bulk material behavior. Then, employing a fairly straightforward cohesive law to describe material behavior in the process zone, one can relate traction to separation. Crack propagation decisions can then be made based on a predefined criticality condition. Cohesive laws can

be embedded into a finite element model as long as one knows the direction of crack growth a priori.

While cohesive zone fracture mechanics is an attractive approach for dealing with solder joint fatigue failure, there are several challenges with regard to the estimation of material parameters and implementation in a computational model that captures the complexity of a typical microelectronic package. Any engineer wishing to solve the problem of solder joint fatigue in a non-empirical manner, is thus faced with a dilemma: while there exist models based on nonlinear fracture mechanics, their practical implementation is not straightforward and often raises more questions than it provides answers. In this paper, we attempt to address this issue by presenting a modeling approach for fatigue crack growth in solder joints which has been successfully implemented specifically to the problem of fatigue in Sn-Pb solder joints [15]. While the approach is inspired by cohesive zone models and resembles them in form, the implementation of the approach is more straightforward. Additionally, to the best of our knowledge, this is the only approach that has been able to successfully predict experimentally observed fatigue crack fronts in solder interconnections that have undergone thermal cycling.

In the sections to follow, a brief review of the use of cohesive zone modeling to address fatigue and focus on application of the theory to solder joint fatigue in particular, is first presented. The origins of the hybrid fracture-damage model are presented in the next section and it is shown to retain a form similar to that used in cohesive zone models while providing greater computational efficiency and ease of implementation. Finally, the applicability and validity of the modeling approach is demonstrated by corroborating simulations to experimentally observed crack growth in solder joints. Results are summarized from previously published work on Sn-Pb solder joints and ongoing work on lead-free solder joints.

The key to greater use of non-empirical approaches lies in the development of computationally inexpensive failure models that may be implemented in a straightforward manner, and well-defined procedures to estimate the required model parameters. Such a non-empirical approach will allow fatigue life predictions via modeling for different package geometries and materials without resorting to full scale thermal cycling tests. Additionally, it will be able to predict acceleration factors for fatigue life during field use. The hybrid fatigue model is developed and presented here, with this overarching goal in mind.

2. Cohesive Zone Fracture Mechanics Approach to Modeling Fatigue Crack Growth

The concept of isolating a region in front of the crack tip as a region loaded with a finite cohesive stress originated in the 1960s [11, 12]. Since then, different laws (at least five) have been proposed to describe the behavior of material in this zone (see Elices et.al. [10] and Brocks et.al. [13] for a complete review). Since the law is phenomenological, there is no fundamental reason to believe that one form of the law is superior to another. More importantly however, whereas the form of the laws may vary, all models assume a traction

separation law that follows the following basic rule: as interfacial separation increases, the magnitude of traction increases, reaches a peak value and then falls to zero. When the traction falls to zero, the material loses its integrity and the crack propagates. Consequently, the area under the traction separation curve can be thought of as being representative of the work that needs to be done to separate material in the process zone. While attempts have been made to connect one of the several forms of the law [14] to the universal binding law proposed by Smith and Ferrante [16], the connection between atomistic observation and macroscopic cracking is a tenuous one. Nonetheless, the traction separation relation derived from the Smith-Ferrante law is among the more popular forms in use and can be written as an equation of the form [15]:

$$T = e\sigma_c \frac{\delta}{\delta_c} \exp\left[-\frac{\delta}{\delta_c}\right] \quad (1)$$

where $e=2.71828$, σ_c is the maximum cohesive normal traction and δ_c is a characteristic opening displacement.

The lack of standardization is not restricted to the definition of the law alone: dealing with mixed mode loading is another area where several ideas have been proposed without a reasonable way to assess them qualitatively. Significantly, very little experimental work has been done to meaningfully corroborate all the hypotheses in the literature regarding the implementation of cohesive zone models. The poor availability of experimental evidence to support cohesive zone modeling theory can perhaps be attributed to one of the biggest challenges faced by researchers who work with these models: estimation of model parameters. Even the most basic cohesive laws for monotonic loading involve two parameters whose estimation is essential in order to describe the law completely.

A key requirement in cohesive zone modeling of fatigue is the incorporation of a damage law to account for degradation of the material. The damage law is typically implemented as a reduction in the load bearing capacity of the material. To cite one example, the expression for damage implemented by de-Andres et.al. [17] in their approach to modeling fatigue using a cohesive zone model was:

$$D = \frac{\phi(\delta_{\max})}{G_c} \quad (2)$$

where $\phi(\delta)$ is the area under the traction separation curve from origin to instantaneous separation (δ) and is essentially a potential derived from Eq. (3) and G_c is the critical energy release rate for crack propagation. At any value of δ_{\max} ,

$$D = 1 - \left(1 + \frac{\delta_{\max}}{\delta_c}\right) \exp\left[-\frac{\delta_{\max}}{\delta_c}\right] \quad (3)$$

Cohesive zone models have been recently applied to the problem of solder joint fatigue [18, 19]. Yang et.al. [18] considered rate-independent plasticity for representing solder behavior and simulated solder joint shear in a two-dimensional model of a single solder joint. A pure-shear (mode II) cohesive law was implemented as a damage evolution law which was a power-law function of the

accumulated plastic strain. The accumulated damage had the effect of reducing the effective shear stress to a level where decohesion was defined. The absence of an explicit traction-separation law raises the question whether this is a cohesive zone modeling approach at all, but the more important practical limitations of this work are the assumption of rate independence of material behavior and the application to a two-dimensional, rectangular joint.

Abdul-Baqi et.al.'s [19] modeling approach incorporates a simplified version of Roe and Siegmund's [20] model and assumes that cohesive zones are embedded at not just the solder joint-pad interface, but also along phase boundaries within the joint. The bulk of the solder joint was assumed to be elastic for simplicity and the computational models were two-dimensional, single solder joints. The need to account for damage at phase boundaries is arguable, given that fracture almost always takes place at the interface of the solder-joint and the pad. The parameters in this work were selected arbitrarily and no realistic experimental scenarios were simulated.

Clearly, the application of cohesive zone models to simulating fatigue crack growth is in its early stages and this is even more so the case for solder joint fatigue. Nonetheless, due to the fundamental requirement of a failure model in the process zone (with behavior different from the bulk material), it is clear that there are several challenges associated with characterizing the material behavior in this process zone. Additionally, the implementation of cohesive zone laws is challenging and in the case of complex three-dimensional microelectronic package simulations, may well be computationally prohibitive. Finally, while the exclusion of the cohesive zone from the surrounding material allows for meaningful computational implementation, it disconnects the failure zone from inherent material behavior. In materials such as solder alloys, which demonstrate complex rate-dependency, microstructural evolution (aging) etc., the isolation of the failure zone from the complex evolution of the material itself may introduce inaccuracies in the model predictions.

The hybrid fracture-damage model, which is the focus of this work, addresses the challenges discussed above. It achieves this primarily by relating damage in the solder joint to the *inelastic strains* that are computed at *every material point* in the joint. Since the inelastic strains are the end result of the material's response to the environmental conditions as interpreted by the constitutive model, complexities of rate dependency, microstructure evolution etc., do not affect the validity of the damage law. In other words, the validity of the hybrid model is only limited by the validity of the constitutive model used for describing the behavior of the material undergoing failure.

3. A Weibull perspective on cohesive zone models

In this section, we discuss the important aspects of the hybrid model and show how the model resembles popular cohesive zone models and achieves the same objectives without resorting to complicated forms and practically hard-to-estimate model parameters.

As mentioned previously, the hybrid modeling approach is developed from the use of Weibull functions to estimate the damage at every material point in the structure undergoing fatigue. Weibull functions [21] have been used successfully for decades to describe failure in a wide variety of applications including failure in microelectronic packages. The Weibull probability density function (PDF) is essentially an exponential, two-parameter equation of the form:

$$f(x) = \frac{\beta}{\eta^\beta} x^{\beta-1} \exp[-(\frac{x}{\eta})^\beta] \quad (x \geq 0) \quad (4)$$

$$= 0 \quad (x \leq 0)$$

where η and β are constants, typically called characteristic life and shape parameter, respectively.

Thus, given a Weibull distribution of the form in Eq. (4), one can completely describe the Weibull PDF if one knows the values of these two parameters. The attractive feature of the Weibull distribution is that by selecting the appropriate parameters, a wide variety of distributions can be approximated with satisfying accuracy. We postulate here that the Weibull PDF may be used to describe behavior at any point in a ductile material undergoing fatigue. In other words, Eq. (3) may be considered a traction-separation law of the form:

$$T = \frac{\beta}{\eta^\beta} \delta^{\beta-1} \exp[-(\frac{\delta}{\eta})^\beta] \quad (5)$$

There is clearly a striking similarity between the forms of the equations derived from the Weibull distribution, Eq. (5) and Smith-Ferrante's universal binding law in Eq. (1). Both equations are exponential and involve two parameters that determine the shape and size of the traction separation curve, as is seen clearly in Fig. 1. Additionally, the existence of several forms of traction-separation relationships in the literature is suggestive of the fact that the exact form of the equation is not a critical issue as long as it follows the increasing-decreasing traction behavior and is completely described by two parameters. The Weibull PDF meets both these criteria and has proven applicability to a wide variety of fatigue failures.

Whereas the traction-separation law in Eq. (5) adequately describes material response in the process zone, it does not by itself account for material degradation in the process zone (due to micromechanical effects such as microcracking and void growth). The area under the traction-separation curve can be related to the degradation through the introduction of a damage measure. This is a readily implemented concept in Weibull functions where the cumulative distribution function (CDF) corresponds to the area under the Weibull PDF. The Weibull CDF is given as:

$$F(x) = 1 - \exp[-(\frac{x}{\eta})^\beta] \quad (6)$$

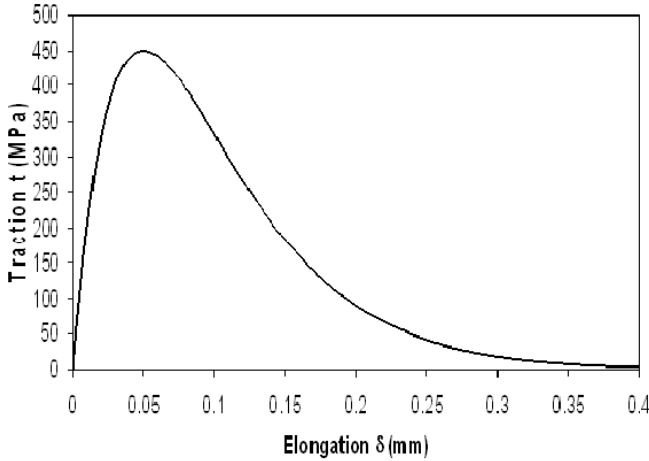
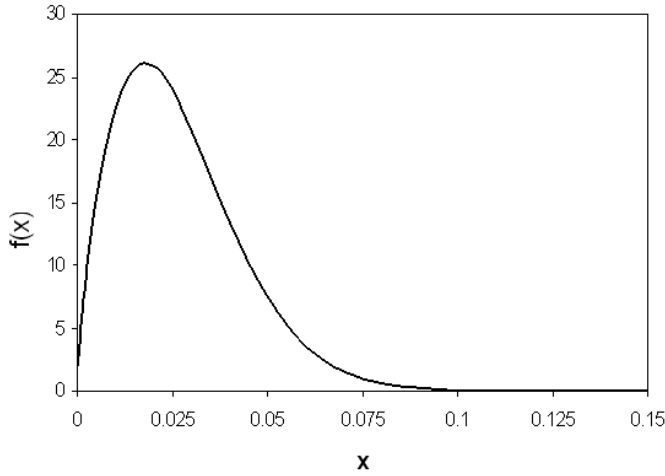


Figure 1. Typical form of the Weibull PDF (left) and the traction-separation law derived from the Smith-Ferrante law (right). The forms are clearly very similar.

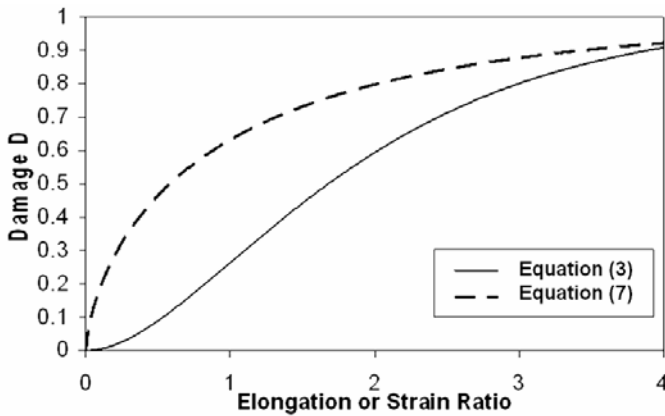


Figure 2. Damage accumulation as a function of elongation ratio [15]

At a given value of x , the CDF represents the area under the PDF curve from the origin up to that value of x . This CDF can be thought of as a measure of damage as:

$$D = 1 - \exp\left[-\left(\frac{\delta}{\eta}\right)^\beta\right] \quad (7)$$

Eq. (7) is plotted along with Eq. (3) (the damage law implemented by de-Andres et.al. [17]) in Fig. 2 for typical

parameter values. Again, it is clear that the mathematical forms of the two damage relationships are similar. Eq. (7) relates damage to the separation of the material point at which damage is being evaluated. For ductile materials, a direct relationship may be postulated between inelastic strains and this separation. The usage of a strain measure instead of crack opening displacement is motivated by the fact that it potentially eliminates the need for dealing with mixed mode loading conditions, where displacements are a combination of opening and shear modes. Inelastic strains are readily computed in a finite element model and capture adequately the creep response of solder alloys, given a valid constitutive model that describes the solder alloy in question.

Eq. (7) can thus be rewritten in terms of total inelastic strain as:

$$D = 1 - \exp\left[-\left(\frac{\zeta}{\zeta_c}\right)^\beta\right] \quad (8)$$

where ζ is the total inelastic strain, ζ_c (representing a characteristic strain) and β are material constants. As with almost all damage accumulation models, it is computationally inefficient to estimate damage every cycle, though this is certainly feasible. To alleviate the computational expense, a one-term Taylor series expansion may be used to extrapolate the damage state and advance the crack [15, 17] -

$$D_{n+1} \approx D_n + \frac{\partial D}{\partial N}\bigg|_n (N_{n+1} - N_n) \quad (9)$$

where N_{n+1} and N_n are the number of cycles of fatigue life at the end of $n + 1$ and n iterations, respectively. D_{n+1} and D_n are the values of the disturbance parameter associated with N_{n+1} and N_n cycles. The rate of disturbance change over a cycle $(\partial D/\partial N)_n$ was calculated using finite difference derivatives. The number of cycles for crack advance was calculated by advancing the disturbance to critical state, that is, by determining the number of cycles when D_{n+1} equals D_c , a predetermined estimate for critical damage. While one may argue that this is strictly not a cycle-to-cycle propagation of cracks due to cyclic fatigue, this is only a question of convenience; it is computationally prohibitive to simulate every cycle in complex systems such as electronic packages undergoing several thousands of cycles to failure.

Hence, at its essence, the hybrid model may be thought of as a cohesive zone model with a traction separation law that is derived from Weibull functions. As a result, all the same benefits that are attributed to cohesive zone models will also apply to the hybrid model. The two key challenges in traditional cohesive zone modeling are the need for special elements in a finite element setting and the estimation of material parameters. These challenges can be readily resolved with the hybrid modeling approach. The requirement for user elements may be done away with by using multi-point constraints, which are released to propagate the fatigue crack [15]. The estimation of material parameters ζ_c and β is relatively easy. Whereas it is possible to obtain these parameters from cyclic tests done on bulk samples [15, 22, 23], an alternative approach is to make advantage of the fact that inelastic strains can be estimated through finite element

models. This approach can be coupled to experimental observations to estimate the parameters that capture the evolution of the crack front correctly. This inverse approach of relating computed inelastic strains to experimentally observed crack fronts is explained in greater detail in the following section, where the hybrid modeling approach is applied to predicting the fatigue life of lead-free solder joints.

4. Model Validation

In this section, validation of the hybrid model for two different structures and material systems is presented. The results from the application of the model to lead-free solder joints are discussed first, including a study validating some of the assumptions in the modeling approach and a novel inverse approach for estimating the required material parameters. The results of applying the hybrid model to making predictions on the fatigue life of Sn-Pb solder joints are then summarized, the details can be found in reference [15].

A test specimen consisting of four solder joints that were hold together by two square alumina substrates at the four corners was designed, as shown in Fig. 3 (a). Fatigue damage was induced in the solder joints using a thermoelectric (peltier) device which was controlled to cause anisothermal conditions. One side of the specimen was placed on the peltier device which cycled between 0 and 100°C. The other side of the specimen was exposed to the ambient. The temperature cycle profile was applied over a total of 13 minutes, with one minute ramp periods (up and down), a ten minute hot dwell and a one minute cold dwell. Details of the specific test setup used can be found in Setty et. al. [25].

Subjecting only one side to the thermal cycle creates a temperature difference between the top and bottom substrates, which subsequently results in the differential expansion of the two substrates. It is this differential expansion, coupled with the inherent creep behavior of the solder alloy that caused fatigue damage of the solder joint. For this particular experiment, identical specimens were tested on the same Peltier device and removed after 411, 621 and 807 cycles for analysis using the commonly employed dye-and-pry technique. The progress of the crack is clearly visible in Fig. 3 (b).

To estimate material parameters and subsequently simulate fatigue crack growth, it is critical to obtain a complete description of the inelastic strain in the solder joint and its evolution during fatigue cycling. In general, the distribution of inelastic strain for a given loading condition will be dependent on the geometry and constitutive behavior of the structure under investigation and the extent of crack growth. A quarter of the test specimen (due to symmetry) was constructed as a finite element model in ABAQUS, version 6.6. The different structural levels of the model are shown in Fig. 4.

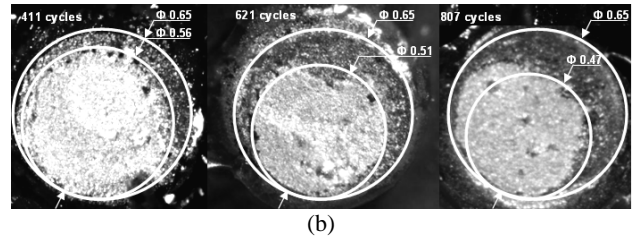
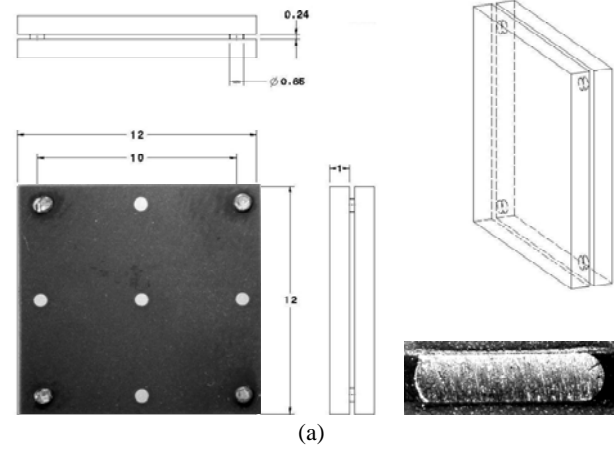


Figure 3. (a) Test specimen dimensions, inset shows cross-section of the solder joint (b) Crack fronts obtained as a result of thermomechanical fatigue imposed on solder joints, followed by red dye penetration. Results shown for (from left to right) 411, 621 and 807 10-minute cycles between 0 and 100°C. The images were processed and crack fronts measured using Scion Image [24]. (All dimensions in mm).

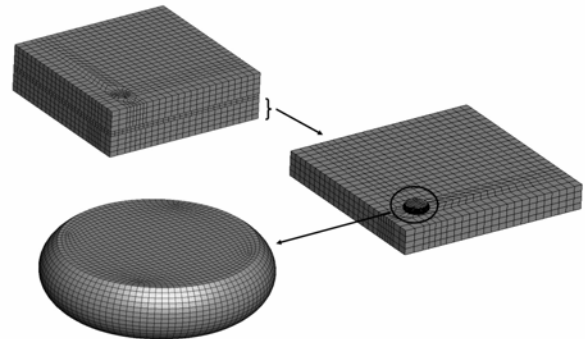


Figure 4. Finite element model of a quarter of the specimen assembly and the refined mesh of the solder joint

The model contained a total of 24636 eight-node brick elements. The simulation was performed in two stages: the first stage simulated the transient heat transfer to obtain temperature information for all points in the structure. In the second stage, the temperatures obtained from the output of the previous stage were used as boundary conditions and the thermomechanical response was simulated as a quasi-static analysis with time-dependent material response. Symmetry conditions were applied to the symmetry planes and the central node at the bottom was constrained in all directions to prevent any rigid body motion. The thin gap between the

alumina coupons was modeled with elements to represent the thermal conductivity of air.

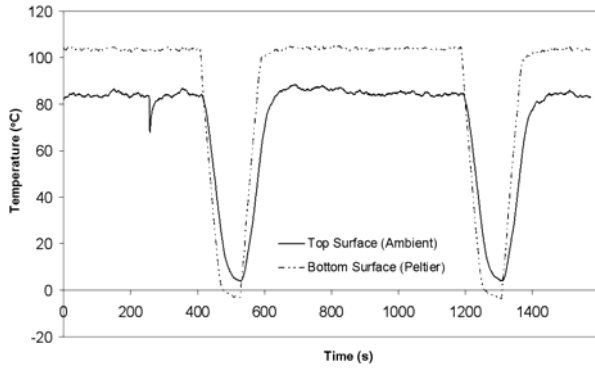


Figure 5. Thermocouple measurements for top (exposed to ambient) and bottom (in contact with Peltier device) of specimen. These profiles were used as isothermal boundary conditions in simulation.

Thermocouples were used to estimate and control the temperature profiles on the two outer surfaces of the sample, one of which was placed directly on the heating device (peltier), the other was exposed to the ambient but experienced a thermal profile due to its proximity to the peltier device. The experimentally measured profiles of the top and bottom surfaces of the test specimen are reproduced in Fig. 5. These temperature profiles were introduced in the finite element model as isothermal boundary conditions on the respective surfaces of the specimen.

The solder interconnection was modeled as a truncated sphere. The joint is held between two 20 μm thick circular copper pads which are located in the alumina coupons. Material properties for alumina and copper were obtained from the manufacturer. The solder, a lead-free alloy of the composition 95.5 % Sn, 3.8 % Ag and 0.7 % Cu (by weight), was modeled using a time hardening creep model that was developed by the authors and is published separately in [2], where a specimen identical to that shown in Fig. 3 (a) was used in a double lap shear arrangement to develop the constitutive model. Since solder alloys undergo significant creep at the temperatures under consideration, it is essential to have an accurate model that can correctly estimate the evolution of inelastic strains as a function of time and temperature. Finally, the solder interconnection was kept constrained to the copper pad using multi-point constraints. The propagation of the fatigue crack was modeled by freeing these constraints in the nodes corresponding to the cracked area.

For simulation of the fatigue crack, the parameters ζ_c and β in Eqn. (8) need to be estimated. Towashiraporn et. al. [15] used parameters estimated by Desai et. al. [22], who in turn used experimental data from cyclic tests done on Sn-Pb solder by Solomon [23]. Here, we propose a coupled experimental-modeling approach that involves tracking crack fronts and studying the evolution of plastic strains in the cracked structure. An examination of the growth of the fatigue crack in the solder joint revealed that the intact area enclosed by the crack front resembled a circle whose diameter reduced as the number of fatigue cycles increased, as shown in Fig. 3 (b).

We thus postulate that the shape of the crack front is such that it encloses a circle whose diameter, at least in the preliminary stages of crack growth, reduces at a constant rate, or:

$$\frac{d\phi}{dN} = \text{const.} \quad (10)$$

where ϕ is the diameter of the circle enclosed by the crack front, corresponding to the intact area in the joint and N is the number of fatigue cycles. With this assumption, and measurements made in Fig. 3 (b), a crack growth rate (along the diameter) of 22 $\mu\text{m}/\text{cycle}$ was estimated, which is expected to be valid for the first 800 cycles at least.

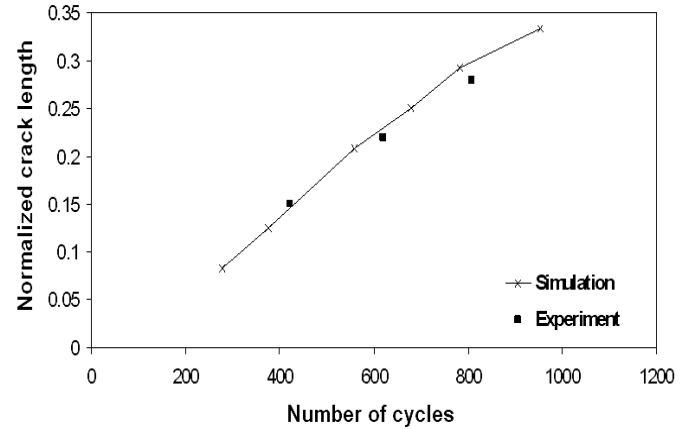
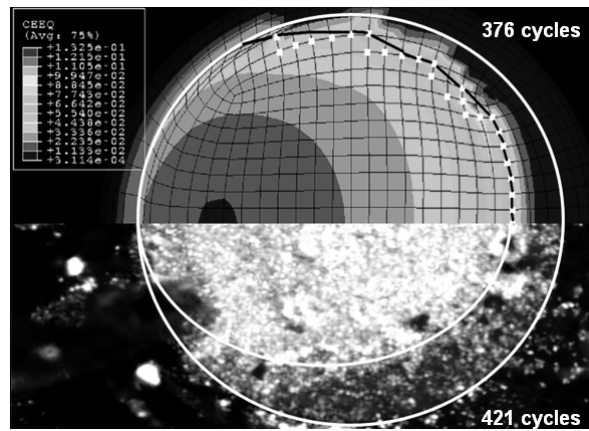
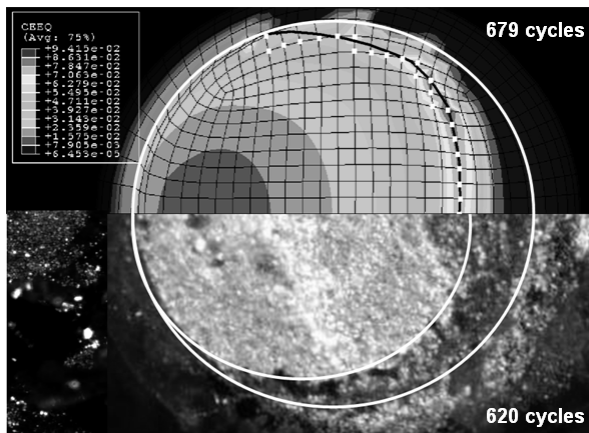


Figure 6. Comparison of experimentally observed and numerically predicted crack fronts

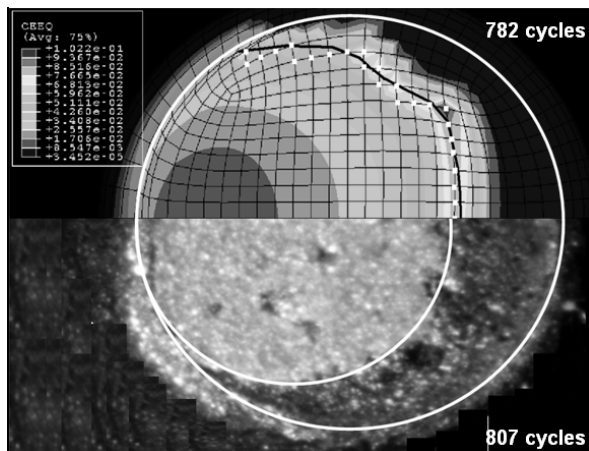
For the estimation of the material parameters, two different models were constructed. The first represented the intact solder joint, where all the nodes between the joint and the pad were tied together. The second model, on the other hand, represented the solder joint after 100 fatigue cycles. For this, the number of nodes with tie constraints were reduced to represent the expected crack configuration after 100 cycles, using the previously mentioned assumption of constant rate of crack growth along the diameter. The lower side of the joint, which was attached to the substrate that was exposed to the higher temperature, was selected for representing the crack surface, in line with experimental observations. This is to be expected, since the lower side of the joint experiences slightly higher temperatures and accumulates creep quicker as a result. Thus, at every material point at the interface, the inelastic strains were computed for two different configurations, corresponding to the intact joint and one that had a crack corresponding to that expected from experimental observation. Substituting Eq. (8) in Eq. (9), an expression relating the accumulated damage to inelastic strains can be obtained for the two models constructed. Therefore, for any two points along the crack front, we can obtain a pair of equations and solve simultaneously for the two parameters, ζ_c and β , which were obtained as 23.55 and 0.76, respectively.



(a)



(b)



(c)

Figure 7. Comparison of experimentally observed and numerically predicted crack fronts for different fatigue cycles. The white squares correspond to the first set of intact tie constraints ahead of the crack front.

Once the parameters were obtained, the simulations were performed and correlated with experimentally observed crack fronts. A plot of the crack growth for the first 1000 cycles as simulated is compared to experimentally measured values in Fig. 6. Figs. 7 (a) to (c) show a qualitative comparison between the actual crack fronts predicted via simulation and observed experimentally – the error in predicted number of

cycles is under 10% and the correlation of the shape of the crack front is satisfactory.

Acknowledgments

This study was partially supported by the Semiconductor Research Corporation (SRC) and by the National Semiconductor Corporation under SRC Tasks 1181.001 and 1394.001. The authors are grateful for this support. The authors are thankful to Drs. Tz-Cheng Chiu, Vikas Gupta and Jeff Zhao of Texas Instruments for providing the test specimen (shown in Figure 4) that made the experimental aspects of the study possible.

References

1. Plumbridge, W.J., "The analysis of creep data for solder alloys," *Soldering & Surface Mount Technology*, Vol. 15, No. 1 (2003), pp. 26–30.
2. Bhate, D., Chan, D., Subbarayan, G., Chiu, T.C, Gupta, V., Edwards, D., "Creep and Low Strain Rate Behavior of Sn3.8Ag0.7Cu and Sn1.0Ag0.5Cu Alloys: Development of Valid Constitutive Models," submitted to *IEEE Transactions on Components and Packaging Technologies*.
3. Ma H., Suhling, J.C., Lall, P., Bozack, M.J., 2006, "Reliability of the Aging Lead Free Solder Joint," *Proc. Electronic Components and Technology Conference*, 2006, pp. 849-864.
4. Lee, W.W., Nguyen, L.T., Selvaduray, G.S., "Solder joint fatigue models: review and applicability to chip scale packages", *Microelectronics Reliability*, Vol. 40, No. 2 (2000), pp. 231-244.
5. Paris, P.C., Gomez, R.E., Anderson, W.E., , "A rational analytic theory of fatigue," *The Trend in Engineering*, Vol. 13, No. 1 (1961), pp. 9-14.
6. Anderson, T.L., 2005, *Fracture Mechanics: Fundamentals and Applications*, 3rd Ed., CRC Press, Boca Rotan, FL.
7. Ritchie R.O., "Mechanisms of fatigue-crack propagation in ductile and brittle solids," *International Journal of Fracture*, Vol. 100, No. 1 (1999)
8. Wells, A.A., "Unstable crack propagation in metals: cleavage and fast fracture," *Proc. Crack Propagation Symp. Vol.1 (1961)*, Paper 84. Cranfield, UK.
9. Rice, J.R., "A path independent integral and the approximate analysis of strain concentration by notches and cracks," *J. Appl. Mech.*, Vol. 35 (1968), pp. 379-386.
10. Elices M., Guinea G. V., Gomez J. ; Planas J., "The cohesive zone model: advantages, limitations and challenges, *Engineering fracture mechanics*, Vol. 69, no. 2 (2002), pp. 137-163.
11. Dugdale, D.S., "Yielding of steel sheets containing slits," *J. Mech. Phys. Solids*, Vol. 8 (1960), pp.100–104.
12. Barrenblatt, G.I., "The mathematical theory of equilibrium of cracks in brittle fracture," *Advances in Applied Mechanics*, Vol. 7 (1962), pp.55–129.
13. Brocks, W., Cornec, A., Scheider, I., "Computational aspects of nonlinear fracture mechanics", *Comprehensive Structural Integrity*, Vol. 3 (2003), pp. 127-209.

14. Needleman, A., "An analysis of decohesion along an imperfect interface," *International Journal of Fracture*, Vol. 42 (1990), pp. 21–40.
15. Towashiraporn P., Subbarayan G.S., Desai C.S., "A hybrid model for computationally efficient fatigue fracture simulations at microelectronic assembly interfaces", *International Journal of Solids and Structures*, Vol. 42 (2005), pp. 4468-4483.
16. Rose, J.H., Smith, J., Ferrante, J., "Universal binding energy curves for metals and bimetallic interfaces", *Physical Review Letters*, Vol. 47, No. 9 (1981), pp. 675-678.
17. de-Andre´s, A., Pe´rez, J.L., Ortiz, M., Elastoplastic finite element analysis of three-dimensional fatigue crack growth in aluminum shafts subjected to axial loading. *Int. J. Solids Struct.* Vol. 36 (1999), 2231–2258.
18. Yang, Shim, Spearing, "A cohesive zone model for low cycle fatigue life prediction of solder joints", *Microelec. Engg.*, vol. 75 (2004), pp. 84-95.
19. Abdul-Baqi, Schreurs, Geers, "Fatigue damage modeling in solder interconnections using a cohesive zone approach", *International Journal of Solids and Structures*, vol. 42 (2005), pp. 927-942.
20. Roe, K.L., Siegmund, T., "An irreversible cohesive zone model for interface fatigue crack growth simulation," *Eng. Fract. Mech.* Vol. 70 (2003), 209–232.
21. Weibull, W.A., "A statistical distribution function of wide applicability," *Appl. Mech.*, Vol. 18 (1951), pp. 293–297.
22. Desai, C.S., Chiu, J., Kundu, T., Prince, J.L., "Thermomechanical response of materials and interfaces in electronic packaging: Part I— Unified constitutive models and calibration," *ASME J. Electron. Packag.* Vol. 119 (1997), pp. 294–300.
23. Solomon, H.D., "Low cycle fatigue of 60/40 solder plastic strain limited vs. displacement limited testing," *Proceedings of ASME Electronic Packaging: Mater. Process.*, (1985), pp. 29–47.
24. Scion Image, Scion Corporation, www.scioncorp.com
25. Setty, K., Subbarayan, G., Nguyen, L., "Powercycling Reliability, Failure Analysis and Acceleration Factors of Pb-free Solder Joints", *Proc. Electronic Components and Technology Conference*, 2005, pp. 907-915.